JOURNAL OF MATERIALS SCIENCE 32 (1997) 5583–5592

Preparation and characterization of high surface area alumina–titania solid acids

G. S. WALKER, E. WILLIAMS, A. K. BHATTACHARYA
Centre for Catalytic Systems and Materials Engineering, Department of Engineering, University of Warwick, Coventry CV4 7AL, UK

As part of a systematic study of solid acids, a series of high surface area single-phase alumina–titania mixed oxides were prepared. These materials were found to have higher surface areas, greater porosity and enhanced specific surface acidity than comparable alumina-titania solid acids reported in the literature. The thermal stability of the phases and their textural and physicochemical properties have been studied over a range of Al/Ti compositions and for calcinations up to 1000 °C. The samples were characterized by differential thermal analysis–thermogravimetry, X-ray diffraction, nitrogen physisorption and X-ray photoelectron spectroscopy. Surface acidity was measured by temperature programmed desorption and *in situ* Fourier transform-infrared spectroscopy, using ammonia as a probe molecule. The strength and density of the acid sites were proportional to the Ti-content.

1. Introduction

Aluminium trichloride and sulfuric acid are extensively used as homogeneous acid catalysts. However, both acids are toxic and environmentally hazardous, making them difficult to handle and to dispose of the waste. A solution to these problems is to use a solid acid which is itself less hazardous than the acids used and can be easily separated from the waste effluent. One such material is alumina–titania which is reported to have both acid and base sites [1–11] at the surface. There is also interest in the use of alumina–titania mixed oxides as supports for transition metal catalysts [4–6, 12].

Reports in the literature on these systems mostly concentrate on the surface acidity of the materials and how this is affected by the Al/Ti composition and the precursor used [2–5]. A factor often not addressed is the heterogeneity of the materials. Alumina–titania is often prepared by coprecipitation or impregnation which will yield materials with multiple phases. These papers also report the properties found for one calcination temperature (typically 500 °C). Often catalytic reactions are more economically viable at elevated temperatures and for such reactions, catalysts which retain their surface area, porosity and catalytic properties at higher temperatures, are required. Two reports did study the change in properties of alumina–titania with temperature. The structural and acidic properties of alumina–titania oxides prepared by coprecipitation from chloride salts were measured at various calcination temperatures (400–900 °C) [2]. However, chloride contamination is inevitable in routes based on chloride salts and is a well-known catalyst poison. The other study looked at titania-rich mixed oxides and found that they sintered to a lesser extent than pure titania and that the anatase to rutile transformation occurred at higher temperatures for the mixed oxides (900–980 °C) than for pure titania (560 °C) [13]. These mixed oxides were prepared by adding a dispersible boehmite sol (AlOOH) to a titania sol, which when dried produced an intimate physical mixture. Both studies showed that for these mixed phase samples, stability to sintering increased with alumina content.

The aim of the work reported here was to prepare single-phase alumina–titania materials which retained their properties to high temperatures. A solid solution should have enhanced thermal stability through inhibiting phase separation and thus inhibit the sintering of the single metal oxides. Having homogeneous samples will also maximize the Al–Ti interaction. Samples were prepared by the alkoxide sol–gel route because the method produces materials with significant advantages for technological applications in this area. Cogels produced by this method are, in general, more homogeneous mixtures than those obtained by coprecipitation, and the porosity can be controlled by the preparation conditions [14–16]. Unlike previously reported literature, this paper reports the preparation of monophasic alumina–titania solid acids, with high and controllable surface area and porosity. These properties are retained to high temperatures and are resistant to sintering at elevated temperatures. Furthermore, the materials are prepared chlorine-free, which is important for the purposes of the present study, as mentioned above.

The systematic study concentrates on alumina-rich oxides because of their greater thermal stability [2, 13]. Of particular interest are the effects arising from the substitution of titanium for aluminium, the

0022–2461

structural properties and the surface acidity. By correlating these effects, we seek to gain an understanding of the principles affecting surface acidity. Differential thermal analysis–thermogravimetry (DTA–TG) was used to identify the formation of oxides from the alcogels. The structural and textural properties were measured by nitrogen physisorption and X-ray diffraction (XRD). X-ray photoelectron spectroscopy was used to characterize the surface chemistry, and surface acidity was measured using ammonia as a probe molecule; the adsorbed ammonia was characterized by temperature programmed desorption and *in situ* Fourier transform-infrared spectroscopy (FT-IR).

2. Experimental procedure

2.1. Preparation

The alcogels were prepared by the hydrolysis of aluminium isopropoxide (98%, Aldrich) and titanium (IV) isopropoxide (97%, Aldrich). The same procedure was used for the single and mixed metal preparations, which aimed to make enough gel to produce 0.05 moles of oxide upon calcination. Aluminium alkoxide followed by titanium alkoxide (in the desired proportions) were transferred to a flask under dry nitrogen and weighed. After adding 80 ml isopropanol to the flask, the mixture was heated up under nitrogen to dissolve the aluminium isopropoxide and then refluxed overnight. The hydrolysis was carried out by adding a water/isopropanol mix drop-wise using a syringe pump to the refluxing alkoxide solution whilst vigorously stirring the contents of the flask. The addition took an hour and a 50% excess of water was used. After the addition, the mixture was stirred and refluxed for a further hour. The alcogel was collected by removing as much of the solvent as possible using a Buchi rotary evaporator with a bath temperature of 30 °C. Some alumina samples were dried by slow evaporation at room temperature in a fume cupboard. The solid gel was dried in an oven overnight at 105 °C. The DTA–TG results were used to select calcination temperatures and the alcogels were calcined at these temperatures for 6 h in static air, using a muffle furnace. Samples were loaded in alumina boats and heated at a rate of $1\,^{\circ}\mathrm{C\,min^{-1}}$ to the required temperature.

2.2. Thermal analysis

Simultaneous differential thermal analysis (DTA) and thermogravimetric analysis (TGA) of the samples was carried out using a Polymer Laboratories STA1500 thermal analyser. The samples ($\sim$ 12 mg) were heated under flowing air up to 1500 °C using a ramp rate of $10\,^{\circ}\mathrm{C\,min^{-1}}$.

2.3. Powder XRD

X-ray powder diffraction patterns were recorded on a Philips PW1710 diffractometer using CuK_α radiation with a nickel filter. Diffractions were measured for 2θ values from 10°–80° with a scanning speed of $0.25^{\circ}\,\mathrm{min^{-1}}$.

2.4. Surface area and porosity measurements

The surface area and porosity of the samples were measured by nitrogen physisorption, using a Micromeritics ASAP 2000. The samples were pre-treated by degassing at 200 °C until the pressure was < 2 mtorr ($\sim$ 12 hs; 1 torr = 133.322 Pa). The BET method was used to calculate surface area and the Barrett, Joyner and Halenda (BJH) model for pore volume distribution (the adsorption results were used).

2.5. TPD

Alcogel samples ($\sim$ 0.2 g) of particle size 200–400 μm were loaded into a stainless steel reactor tube using quartz wool plugs to keep the powder in the middle of the tube. The gas pressure in the reactor was atmospheric and the flow rate for all gases was $50\,\mathrm{ml\,min^{-1}}$. Helium (cp grade, BOC) was dried by passing through a liquid-nitrogen trap; other gases were used as-received. The temperature of the sample was controlled by a Newtronics micro96 temperature controller. Samples were calcined *in situ* under flowing dry air (BOC) at 600 °C for 6 h using a ramp rate of $1\,^{\circ}\mathrm{C\,min^{-1}}$. After calcination, the sample was purged with helium for 1 h at 100 °C prior to adsorbing ammonia (99.9%, Linde) for 30 min at the same temperature. To remove physisorbed ammonia the sample was purged with helium for 4 h at 100 °C. The TPD was carried out under flowing helium using a ramp rate of $10\,^{\circ}\mathrm{C\,min^{-1}}$ heating the sample up to 600 °C. The desorbed ammonia was detected using a Hiden mass spectrometer to sample the exhaust gases. The mass spectrum signal used to detect ammonia was $m/z = 16$, the contribution to this signal from water was removed by subtracting a 0.9% of the $m/z = 18$ intensity. The mass spectrometer was calibrated after each experiment using 1.0 ml pulses of ammonia from a Valco valve.

2.6. IR spectroscopy

A Galaxy 7020 FT–IR spectrometer with an MCT detector was used to collect IR spectra. A Graseby–Specac high-temperature high-pressure cell was used to obtain *in situ* transmission spectra of the samples. The samples were loaded as wafer-thin self-supporting discs. Titania was studied by diffuse reflectance IR spectroscopy using a Graseby–Specac DRIFTS selector and environmental chamber. KBr was found to be a suitable diluent for the DRIFTS experiments (i.e. did not react with ammonia), and was ground with the titania in $\sim 4:1$ ratio. The temperature of the cells were controlled by a Eurotherm 847 controller and gas treatment/supply was the same as for TPD. The oxides were dried by heating to 200 °C for 1 h under dry helium and then cooled to 100 °C. Ammonia was passed over the sample for 30 min at 100 °C, and then purged with helium at the same temperature for 3–4 h to remove the physisorbed ammonia. Spectra were taken of the dried sample and after the helium purge.

2.7. XPS

The powder samples were put into a dish-shaped holder and lightly pressed to give a compacted smooth surface. A Kratos XSAM 800 photoelectron spectrometer was used for the analysis which consisted of scans of the O 1s, C 1s, Ti 2p and Al 2p spectral regions. Primary excitation was achieved with MgK_α X-rays (120 W) and a multichannel detector was used to detect the emitted photoelectrons. The spectrometer was run in the Fixed Analyser Transmission (FAT) mode and at the highest available resolution (1.2 eV). Data processing was performed using the Kratos DS800 software. The spectra for alumina and the mixed metal oxides were referenced to the O 1s position for alumina, 532.7 eV, and the titania spectra were referenced to an O 1s position of 530.7 eV. Previous work has shown that charge referencing using the C 1s peak is unreliable for some metal oxide and mixed metal oxide systems, and that the O 1s peak is a suitable internal reference [17, 18].

3. Results and discussion

The DTA–TG results are given in Table I, and Fig. 1 shows the DTA–TG plots for selected gels. For the titanium alcogel, Fig. 1a, two endotherms were detected with associated weight loss, and this was assigned to loss of water. Towards the end of the second endotherm there was a large exotherm with little change in sample weight, corresponding to a phase change. After the exotherm there was a small broad endotherm with associated weight loss, followed by another sharp exotherm corresponding to a further phase change. There was no further weight loss after the second exotherm and the total weight loss for the sample was 22.3%. At 530 and 830 °C there were two thermal events with no corresponding change in sample weight. These were further phase transformations which would have evolved heat; however, because the exotherms were so small, it was difficult to differentiate them from the change in the DTA baseline. The product after DTA–TG was a yellow powder. The stoichiometry of the gel determined from the sample weight loss was $TiO_2 \cdot 1.25\ H_2O$. Although the gel is expressed as an oxide, it is more likely that it was a hydrated oxyhydroxide.

There are many phases of alumina and the phase produced depends on the precursor structure and heat treatment [19, 20]. The alkoxide preparations produce a boehmite phase [21], γ-AlOOH, which upon heating forms $\gamma \rightarrow \delta \rightarrow \theta$-alumina and finally α-alumina at ~1100 °C [19, 20]. On heating the aluminium alcogel, Fig. 1b, there was an endotherm with loss of sample weight, followed by two exothermic and an endothermic events, all with varying degrees of sample weight loss. At 900 °C there was a change in the DTA signal and finally an exotherm 1180 °C. There was no loss of sample weight during these last two events. The product after thermal analysis was still a white powder but it had sintered greatly. Constant weight was achieved by 650 °C, with a total weight loss of 23.4%. From this it was determined that the sample had 0.35 moles of water per mole of boehmite prior to the experiment. This water was desorbed at 80 °C and the anhydrous boehmite decomposed in three stages forming alumina by 600 °C (assumed to be γ). The phase transformations at 900 °C are probably the conversion of γ-alumina to δ- and θ-alumina. These phase changes are slow and often overlap making them difficult to determine by DTA–TG. Finally the exotherm at 1180 °C was attributed to α-alumina formation.

The mixed metal alcogel DTA–TG results were similar to those for alumina. It was found that with increasing titanium content the changes in rate of weight loss for the TG curves became less discrete. Also, thermodynamic events associated with the formation of alumina decreased in magnitude and some events attributable to the formation of titanium oxide species became more evident. For example, the magnitude of the alumina exotherm at ~ 500 °C decreased with increasing titanium content, and was not detected for the 75:25 sample. Thermal events associated with titania were more easily identified in the DTA–TG plot for the 75:25 sample, Fig. 1d. These events were a large exotherm at 270 °C, attributed to the formation of a titanium oxide network, and a small exotherm at 815 °C, assigned to rutile formation. The temperature of formation of α-alumina decreased with increasing titanium-content. The exotherm at 1035 °C with a shoulder at 950 °C was assigned to the formation of α-alumina (cf. 1180 °C for alumina).

TABLE I DTA-TG results for aluminium–titanium alcogels: exo, exotherm; endo, endotherm; sh, shoulder

Al_2O_3:TiO_2	DTA–TG results (°C), weight loss in parentheses				
100:0	80 endo (9%)	215 exo (3%)	430 endo; 510 exo (11%)		1180 exo
95:5	80 endo (11%)	225 exo (4%)	440 endo (8%)		1170 exo
90:10	80 endo (14%)	200 endo (6%)	450 endo; 510 vw exo (9%)		1170 exo
80:20	95 endo (9%)	200 exo (6%)	350 exo; 490 exo (9%)		1130 exo
75:25	70 endo (15%)	220sh; 270 exo (20%)		815 exo	950 sh 1035 exo
0:100	100 endo (8%)	215 endo; 260 exo (10%)	340 endo; 430 exo (4.3%)	830 exo	
Assignment:	dehydration	alcogel to oxide transformation			α-Al_2O_3 formation

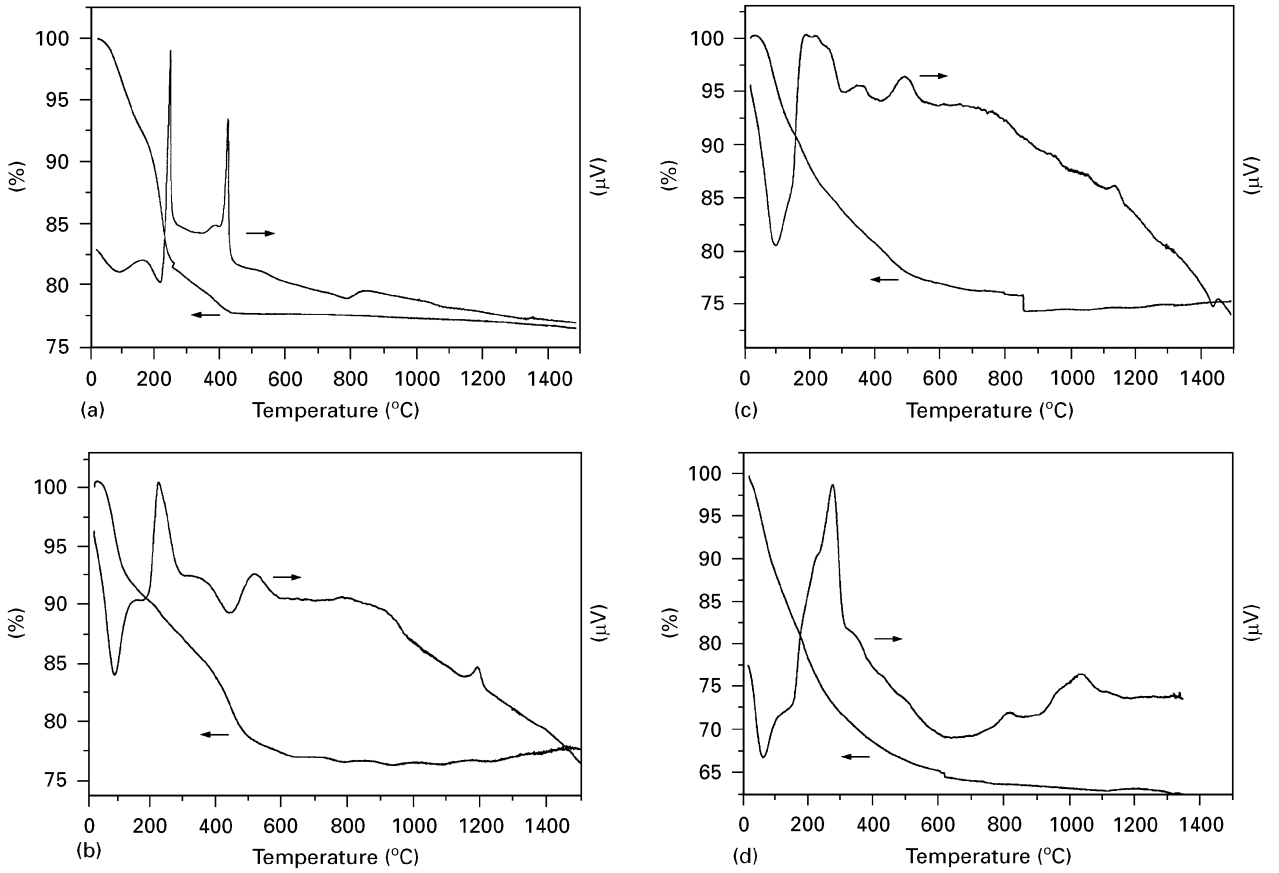

Figure 1 DTA–TG plots for alumina–titania cogels: (a) 0:100, (b) 100:0, (c) 80:20, (d) 75:25.

Fig. 2 summarizes the XRD phase analysis. The titanium alcogel was found to be amorphous, but calcination of gel produced anatase at 400 °C, a mixture of anatase and rutile at 600 °C and was finally converted to rutile by 1000 °C. All the samples were slightly off-white powders. The yellow powder collected after DTA–TG analysis of the titanium alcogel was also rutile. Combining these findings with the DTA–TG results, the titanium alcogel transformed upon heating to an oxide by loss of water (endotherms at 100 and 215 °C) accompanied by the formation of a hydrated anatase phase (exotherm at 260 °C). This was followed by a further loss of water (340 °C) and another phase transformation (exotherm at 430 °C) forming anatase. It is expected that the phase change detected at 430 °C by DTA was fully completed after calcining the gel at 400 °C for 6 h. The onset of rutile formation was detected by DTA at 530 °C and the thermal event at 830 °C may have been caused by loss of lattice oxygen. The latter assignment is supported by the observation that titania slightly deficient in oxygen ($TiO_{1.999–1.990}$) is yellow in colour [22], as was the DTA–TG product. Also, the transformation of rutile from a white to a yellow solid has been detected in air at 900 °C [23].

Powder XRD of the aluminium and mixed metal oxyhydroxide cogels confirmed that they had a boehmite structure. The XRD lines were quite broad and the crystallinity decreased with increasing titanium content. Titania was not detected for any of the mixed metal oxides formed at 600 °C. XRD of the mixed oxides and pure alumina gave diffuse γ-alumina

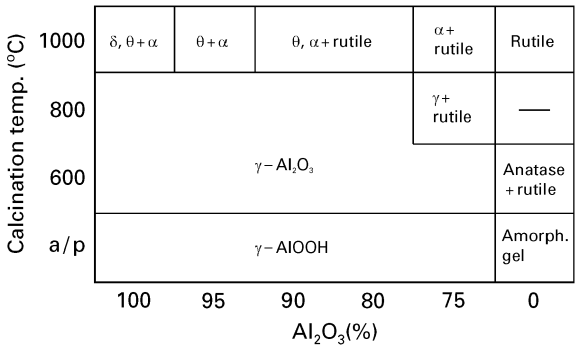

Figure 2 Phases identified by powder XRD for $Al_2O_3:TiO_2$ samples calcined at different temperatures. a/p = uncalcined samples (as-prepared).

patterns, the crystallinity of the products decreasing with increasing titanium content. The incorporation of Ti^{4+} has disrupted the alumina phase, producing a more X-ray amorphous phase. The products formed at 800 °C were also γ-alumina, but were more crystalline than those calcined at lower temperature. Once again, crystallinity decreased with increasing titanium content. The only exception was the 75:25 sample which also gave a rutile XRD pattern. This supports the assignment of the exotherm reported at 815 °C being due to rutile formation.

The materials produced after calcination at 1000 °C were all multi-phase oxides, Fig. 2, the 95:5 sample was the only mixed metal oxide to have no titania phase detected. The alumina phases produced were dependent on the titanium content; as this increased,

so the α-alumina patterns became stronger and the diffraction lines narrower. It would appear that the presence of Ti^{4+} reduced the temperature for the alumina phase changes. The crystallinity of the boehmite can affect the phase transformations, with some less-crystalline boehmites not forming δ-alumina [19]. The increasing amorphous nature of the precursor materials with titanium content indicates that the alumina matrix was disrupted by the inclusion of titanium. It is postulated that this prevented the γ, δ and θ phases from forming properly, and so decreased the activation energy for the alumina transformations.

The XRD results show that the mixed metal oxyhydroxide cogels consisted of titanium cations incorporated in a boehmite matrix. When calcined, these cogels formed a single-phase solid solution with titanium incorporated in an alumina matrix. The solid solutions showed no sign of phase separation up to 800 °C except for the 75:25 sample, which was a mixture of rutile and a γ-alumina-based phase after calcination at 800 °C. Lower titanium content solid solutions underwent separation at higher temperatures and the 95:5 sample showed no sign of phase separation, even after calcination at 1000 °C.

The adsorption isotherms for alumina and titania are given in Fig. 3. The hysteresis loop for the alumina isotherm is characteristic of a substrate with cylindrical pores, while that for the titania isotherm is indicative of either ink-bottle pores or voids between close-packed spherical particles [24]. Titania had little porosity, Table II, and so the sample was most likely a non-porous powder consisting of spherical particles. The isotherms for the mixed oxides were similar to that for alumina. It was found that the uptake of nitrogen at a relative pressure of ~0.85 decreased with increasing calcination temperature indicating loss of porosity.

Titania formed at 400 °C had low surface area, 50 $m^2 g^{-1}$, and little porosity, 0.1 $cm^3 g^{-1}$. Alumina and the mixed metal oxides produced after calcination at 600 °C had surface areas of ~400 $m^2 g^{-1}$ and porosities of ~1.5 $cm^3 g^{-1}$. Many alumina–titania samples reported in the literature [6–8, 11] prepared via the alkoxide route typically have surface areas and porosities of 200–260 $m^2 g^{-1}$ and 1.0 $cm^3 g^{-1}$, respectively. Compared with these, the materials discussed here had much higher surface areas and greater porosity. The enhanced textural properties are, in part, due to the method of drying. It was found that samples dried at room temperature by slow evaporation had lower surface areas (~300 $m^2 g^{-1}$) than those dried under reduced pressure using a rotary evaporator (bath temperature ~30 °C). Even the lower surface-area oxides prepared had significantly greater areas than other preparations reported in the literature. The most likely reason for this is the amount of water used during hydrolysis. The preparations described here used a 50% excess water; however, many literature preparations used up to a 30-fold excess of water. The preparation conditions affect the porosity and surface area of the gels [25–28] and it is reported that water added to undried alumina/silica gels can enhance the porosity of the gel, but that a large amount of water greatly reduced its porosity [16]. We suggest that a large excess of water during hydrolysis has a detrimental effect on the textural properties of the solids produced.

Comparing the samples calcined at 600 °C, the mixed metal oxides had somewhat larger surface areas than pure alumina, Fig. 4 and Table II. Calcination at 800 °C reduced the surface areas for all the samples, but the 75:25 mixed metal oxide had sintered to a much greater extent than the other samples (180 $m^2 g^{-1}$ compared to 250 $m^2 g^{-1}$ for alumina). After calcination at 1000 °C the mixed metal oxides were all lower in surface area than alumina. It can be seen from Fig. 4 that the surface area decreases with increasing titanium content and that for titanium

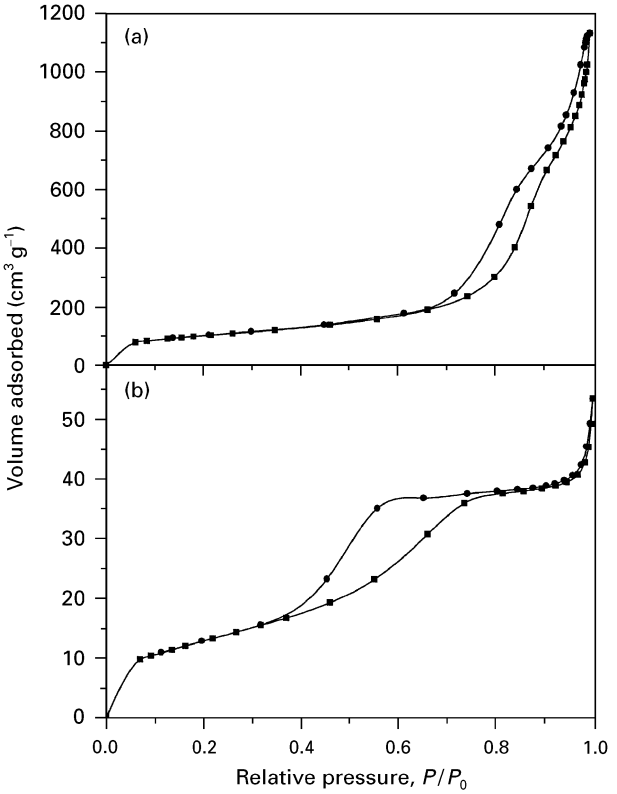

Figure 3 Nitrogen adsorption isotherms for (a) alumina calcined at 600 °C and (b) titania calcined at 400 °C.

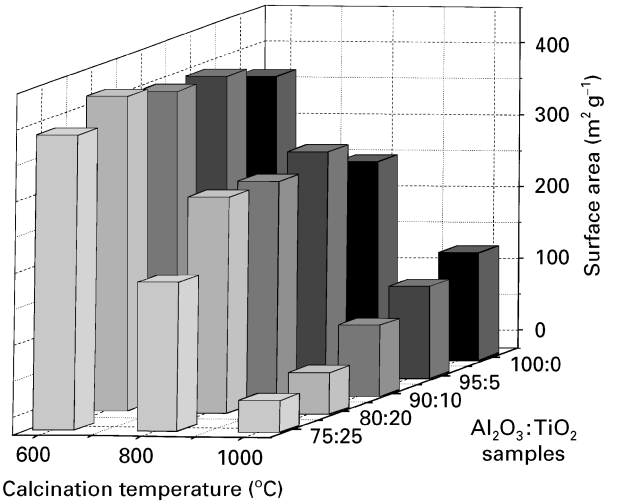

Figure 4 Surface area measured for alumina : titania samples calcined at 600, 800 and 1000 °C.

TABLE II Surface area and porosity for alumina–titania mixed oxides

Sample Al_2O_3 : TiO_2	Calcination temp. (°C)	Surface area ($m^2 g^{-1}$)	Pore vol. ($cm^3 g^{-1}$)	Pore diameter (nm)
100 : 0	600	370	1.6	13, 40–100
	800	250	1.2	15, > 50
	1000	125	0.7	21
95 : 5	600	395	1.8	17, 30–100
	800	290	1.5	18, 40–50
	1000	105	0.7	30–100
90 : 10	600	400	1.5	10, 20–100
	800	275	1.4	20, 50 (sh)
	1000	75	0.5	60–100
80 : 20	600	415	1.4	65, 20–100
	800	275	1.0	10–100
	1000	35	0.1	> 40
75 : 25	600	385	1.2	7, 30–100
	800	180	0.7	11, 20–100
	1000	20	0.1	> 50
0 : 100	400	50	0.1	5

contents of 20% or more, the products were of low surface area (i.e. $< 40 m^2 g^{-1}$).

Similar trends were also found for the pore volumes of the samples, Table II. For the mixed metal oxides, the pore volume decreased with increasing titanium content and it was also found that the porosity decreased with increasing calcination temperature. The most marked loss of porosity was after calcination at 1000 °C. The higher titanium content samples had negligible porosity and the pore volume for the other oxides was half that of the same cogel calcined at 800 °C. It is interesting to note that, excluding the 75 : 25 sample, the mixed oxides had comparable or slightly greater pore volumes than alumina, except when calcined at 1000 °C where only the 95 : 5 sample had similar pore volume.

The pore-size distribution was also affected by titanium content. The predominant pore size decreased with increasing titania for samples calcined at 600 °C. When the samples were calcined at higher temperatures, there was a loss of mesoporosity (2–20 nm). It can be seen from Fig. 5 that mesoporosity was lost with higher calcination temperatures leading to peaks in the plots at 13, 15 and 21 nm after calcinations at

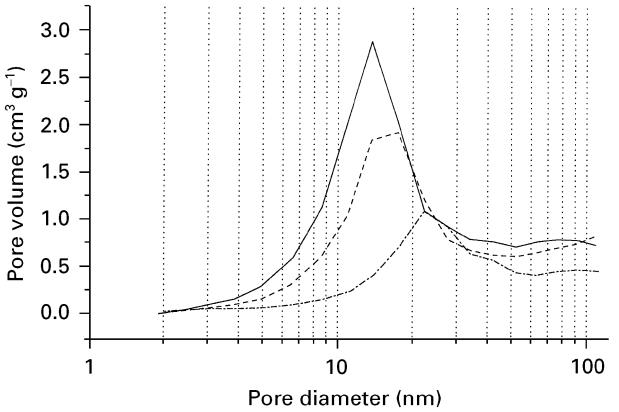

Figure 5 Pore-size distribution for alumina calcined at (——) 600, (– – –) 800 and (— · —) 1000 °C.

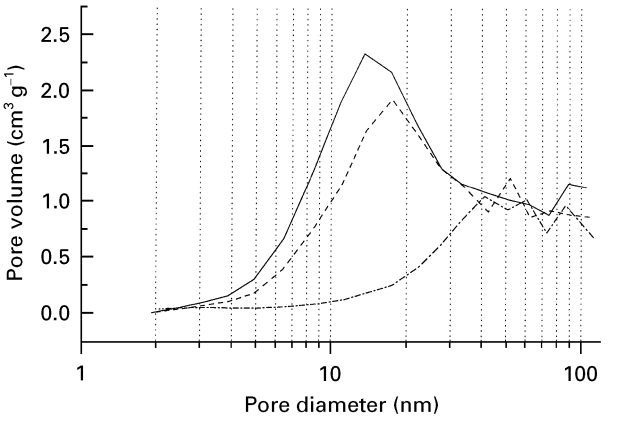

Figure 6 Pore-size distribution for alumina : titania : : 95 : 5 calcined at (——) 600, (– – –) 800 and (— · —) 1000 °C.

600, 800 and 1000 °C, respectively. However, there was very little change in the volume of pores with diameter greater than 20 nm (macropores). For the 95 : 5 sample, Fig. 6, it can be seen that as well as a similar loss of mesoporosity with increasing calcination temperature, there was also fewer 20–30 nm pores at 1000 °C. The 90 : 10 sample was similar but the two samples with greatest titanium content were greatly sintered by 1000 °C, leaving behind negligible porosity. The loss of surface area and porosity of the products coincides with an increase in crystallinity, samples with a well-formed α-alumina phase having the lowest surface area and porosity.

Many acidity measurements in the literature use pyridine as the probe molecule; however, pyridine is a weak base and will only interact with strong acid sites. Lahousse *et al.* found that using 2,6-dimethylpyridine, which is a stronger base than pyridine, they were able to detect by IR, Brønsted acidity at the surface of alumina–titania mixed oxides but only Lewis acidity when using pyridine [11]. However, 2,6-dimethylpyridine cannot coordinate to Lewis sites because of steric hindrance. The use of bases with differing pK_a values to separately characterize Lewis

and Brønsted sites is less than satisfactory because one would be measuring one type of acidity to higher values of pK_a than the other. Thus, we have chosen to use ammonia as the probe molecule as it is a strong base, able to dissociate protons from weaker Brønsted sites and will coordinate to Lewis sites. In order to fully characterize surface acidity, two techniques have been employed, FT–IR to measure the ratio of Lewis to Brønsted sites, and TPD to determine the acid site density and indicate the strength of these sites.

A problem sometimes encountered is the reaction of the probe molecule whilst adsorbed to the substrate. Pyridine has been found to form dipyridyl radicals [29, 30] and pyridine carbanions [29] over basic materials. The anion adsorbs at 1546 cm^{-1} which is coincidental with pyridinium IR bands [29]. In the literature, there is evidence that hydrogen abstraction of ammonia forming amides occurs at elevated temperatures over basic sites [29, 31–33]. IR bands due to these surface amide species are found at 1550–1500 cm^{-1}. Whichever probe is used, careful analysis of the spectra is required to determine if hydrogen abstraction has occurred.

The acid-site density for the oxides calcined at 600 °C was measured by TPD of ammonia and the results are given in Table III. It was found that titania had a higher density of acid sites than alumina, but because the titania had a much lower surface area than alumina it had fewer acid sites per gram of oxide (6.9×10^{-5} compared to 1.5×10^{-4} mol g^{-1}). This is reflected in the TPD profiles for the two oxides, Fig. 7, which have been normalized to 1 g of sample. The TPD profile for titania was a very broad peak at 350 °C, ammonia started to desorb at 150 °C and finished by 550 °C. More ammonia was desorbed from alumina at lower temperatures than titania, forming a TPD peak at 230 °C. Ammonia continued to be desorbed at higher temperatures up to 580 °C, forming a long tail in the TPD plot.

For the mixed metal oxides, the amount of ammonia desorbed increased with increasing titanium content, with the 75:25 sample desorbing a similar amount of ammonia to that from titania. The TPD profile for the 95:5 sample starts off similar to that for alumina but after the peak at 230 °C there are shoulders at 345 and 500 °C. For the other mixed metal oxides, the amount of ammonia desorbed at higher temperatures increased with increasing titanium content, with ammonia still being desorbed at 600 °C. For

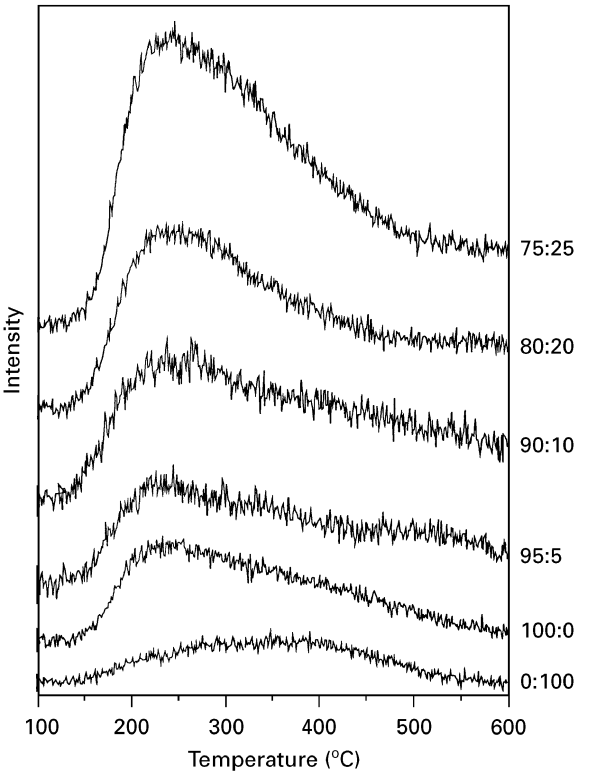

Figure 7 Temperature programmed desorption of ammonia from alumina : titania samples calcined *in situ* at 600 °C. Sample composition is given on the right-hand side of the figure.

the 75:25 sample the TPD profile consists of a large peak at 240 °C, the rate of desorption slowly decreasing with increasing temperature and levelling off at 500 °C.

The IR results for ammonia adsorbed on to the oxides are also given in Table III. Ammonia adsorbed on titania had IR bands at 1594 and 1187 cm^{-1}, indicative of ammonia coordinated to a Lewis acid site [34], see Fig. 8. The spectrum of ammonia adsorbed on alumina had bands at 1608, 1585 (sh) and 1258 cm^{-1} corresponding to Lewis sites and absorptions at 1680, 1470 (sh), 1459 and 1395 cm^{-1} from the ammonium ion (i.e. Brønsted sites) [31, 34]. Ammonia adsorbed on the mixed oxides gave IR bands in the 1615 and 1470 cm^{-1} regions. The band at $\sim$1615 cm^{-1} appears to be comprised of two peaks, one at $\sim$1610 and the other at $\sim$1620 cm^{-1}, superimposing to form a broad peak. There were two peaks n the other region, 1480 and 1455 cm^{-1}, indicative of

TABLE III TPD and *in situ* FT–IR surface acidity results for $Al_2O_3 : TiO_2$ samples calcined at 600 °C.

Sample $Al_2O_3 : TiO_2$	NH_3 desorbed (10^{-7} mol m^{-2})	Coordinated ammonia (cm^{-1})		Lewis : Brønsted
		$\nu_s(NH_3)$	$\nu_{as}(NH_4^+)$	
100:0	3.6	1608, 1585(sh)	1480 (sh), 1459	2:1
95:5	4.2	1624[a]	1483, 1457	3:2
90:10	6.1	1618[a]	1475, 1460	1:1
80:20	6.6	–	–	–
75:25	11	1626[a]	1461[a]	2:1
0:100	14	1594	–	Lewis

[a] wave number corresponds to the absorption maxima of a composite band.

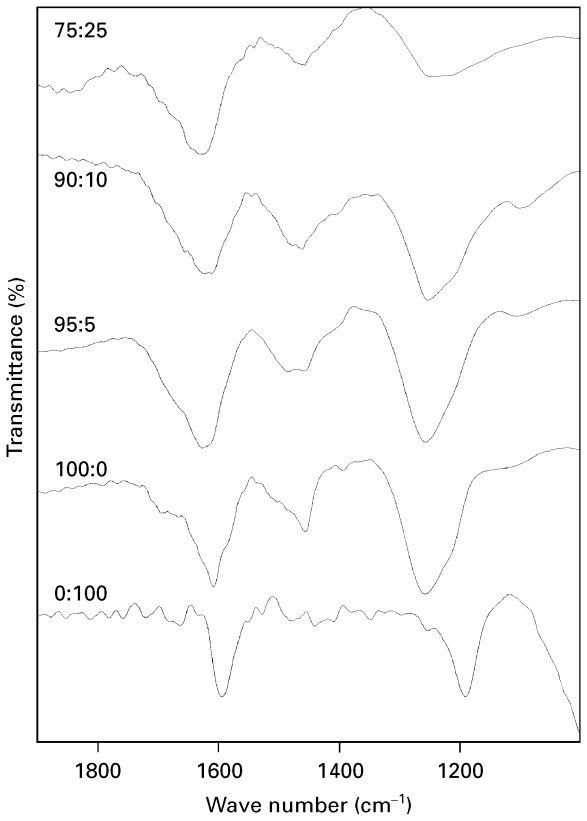

Figure 8 IR spectra of ammonia adsorbed on alumina : titania samples calcined at 600 °C. The spectra for the oxides have been subtracted. Sample composition is given on the left-hand side of the figure.

Brønsted acidity. However, the former band was only a shoulder in the spectrum for the 75 : 25 sample. Amide bands ($\sim$1530 cm^{-1}) were not observed in any of the IR spectra, indicating that ammonia had not dissociated on the surface of the samples.

Using the extinction coefficients for the Lewis and Brønsted IR absorptions (2.6 and 2.0 cm μmol^{-1}, respectively [35]) the ratio of the acid sites can be calculated from the peak areas. The calculated Lewis Brønsted ratios are given in Table III. Both alumina and 75 : 25 sample had twice as many Lewis acid sites as Brønsted, whereas the other two mixed oxides had a slightly higher proportion of Brønsted sites, with the 90 : 10 sample having an equal number of Lewis and Brønsted sites.

From the ammonia adsorption experiments, it has been found that titania has Lewis surface acidity and that these acid sites are of moderate strength (desorption at 350 °C). Alumina had both Lewis and Brønsted acid sites in a 2 : 1 ratio, and there were both weaker and moderate strength sites. The alumina–titania samples had greater acid-site density than pure alumina and the mixed oxides had stronger acid sites than the pure oxides. The acid-site density and number of stronger acid sites increased with increasing titanium content.

It is difficult directly to compare these results with those in the literature because of the different techniques used to measure acidity, giving relative rather than absolute measurements of acidity. It has been found that the number of acid sites decreased with increasing titania content for alumina samples impregnated with titania and the strength of the acid sites was unaffected by the presence of titania [4]. The acidity of materials obtained via coprecipitations is dependent on preparation conditions [10]. It was found that copreciptations using ammonia yielded mixed oxides with the same acidity as alumina, but when urea was used for the precipitation, some of the mixed oxides had a greater number of acid sites than alumina and some sites of higher acid strength. However, there was no real trend between titania content and acidity. In contrast, for the single-phased alumina–titania materials reported here, a clear relationship was found between titanium content and both acid strength and density. Both increased with increasing titanium content.

The XPS technique can, in favourable circumstances, give information about chemical composition and environment. The Al 2p peak position for alumina (Table IV) was in agreement with literature values [36] (75.8 eV) and there was little change detected in the Al 2p position for the mixed metal oxides, 75.6 $\pm$ 0.2 eV. A single Ti 2p peak was detected for the mixed metal oxides and, compared to pure titania was shifted to higher binding energy by 0.8 $\pm$ 0.1 eV. The O 1s signal for the alumina–titania samples was a single peak, no titania O 1s signal was detected for any of the mixed metal samples. The shift in the Ti 2p peak position indicates that the titanium was in a modified environment, suggesting that the cations were homogeneously dispersed throughout an alumina matrix as opposed to a heterogeneous mix of alumina and titania. This is also supported by the O 1s spectra which showed no separate titania features for the mixed metal oxides. These findings corroborate the conclusions from the XRD data that the mixed oxides calcined at 600 °C were single phase.

The Ti 2p shift to higher binding energy indicates that the titanium cations were in an electron-deficient environment compared to that for pure titania, and will therefore be better electron acceptors, i.e. stronger acid centres. This is in agreement with the TPD results which showed that the mixed metal oxides had stronger acid sites than pure titania. The reason for the titanium cations being more electron deficient could be due to the charge imbalance resulting from a titanium (IV) cation located in an aluminium (III) site, or arise from the differing electronegativities of the two cations [37].

TABLE IV XPS results for Al_2O_3 : TiO_2 samples calcined at 600 °C.

Sample Al_2O_3:TiO_2	Al2p BE[a] (eV)	Ti 2p BE[b] (eV)	Surface composition Al_2O_3 : TiO_2
100 : 0	75.6	–	–
95 : 5	75.5	460.2	95 : 5
90 : 10	75.6	460.2	91 : 9
80 : 20	75.7	460.3	75 : 25
75 : 25	75.8	460.4	50 : 50
0 : 100	–	459.5	–

[a]Referenced to alumina O 1s (532.7 eV).
[b]As [a]except pure titania referenced to O 1s BE = 530.7 eV.

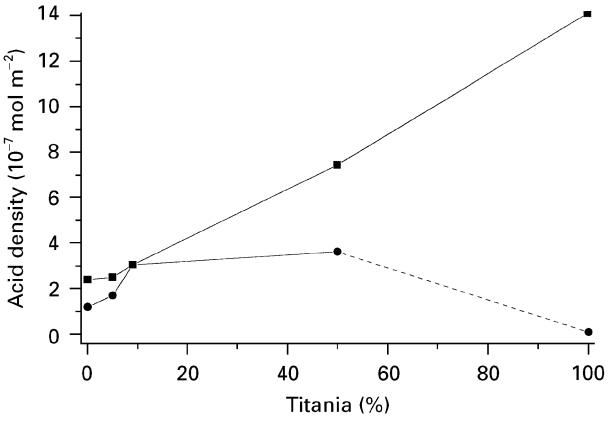

Figure 9 Acid site density versus surface composition for alumina–titania samples calcined at 600 °C: (■) Lewis, (●) Brønsted.

From the surface composition determined by XPS, Table IV, the oxides with up to 20% titania appear to be homogeneous and exhibit no surface separation. Surface enrichment of titania was detected for the sample with a bulk titania content of 25%. The surface enrichment may have been due to ion migration during calcination or to the preparative conditions. The homogeneity of cogels is sensitive to preparative conditions (e.g. mixing and hydrolysis rate) and this may have resulted in the surface enrichment observed.

Comparing surface composition with the acidity results (Table III) shows that the density of acid sites increased with titania content. Lewis and Brønsted acidity is plotted against surface composition in Fig. 9. This plot shows that the Lewis acid-site density increased almost linearly with titania content, whereas the number of Brønsted sites reached a maximum by 10% titania content. A dotted line was used in the Brønsted plot to indicate that the density would not necessarily decrease after 50% surface titania content. Lewis acid density was a function of titanium content, i.e. the substitution of titanium cations into an alumina lattice created Lewis acid sites. However, for Brønsted acidity although there was an initial increase in density with increasing titanium content, a maximum was reached by 10% titania inclusion. The density of Brønsted sites was not related to surface titanium content alone. A Brønsted site also requires a hydroxyl group, and it is postulated that the number of sites was limited by the availability of hydroxyl species. Based on this postulation it is expected that Brønsted site density would remain at a constant level until the surface characteristics became more like titania, i.e. Lewis acidity only, whereupon Brønsted density would decrease with titania content.

4. Conclusion

It has been shown that aluminium–titanium cogels produced single-phase solid acids. It was found that the single phases were retained to high temperature (800–1000 °C) and that the temperature of phase separation was dependent on the titanium content. Apart from titania, the oxides calcined at 600 °C had high surface areas and porosity, almost double that normally reported in the literature. Furthermore, these properties were essentially retained at higher temperatures while the materials remained single phase. The enhanced textural properties were in part attributed to the limited amount of water used in the preparation and the removal of the solvent using a rotary evaporator. For lower calcination temperatures, the level of crystallinity of the oxides decreased with increasing titania content. In contrast, the crystallinity and the amount of α-alumina formed after calcination at 1000 °C increased with increasing titanium content.

The textural properties of the mixed oxides were affected by both composition and calcination temperature. At lower calcination temperatures, the mixed oxides had enhanced textural properties compared to alumina. Pore size was related to the composition of the cogel, i.e. the greater the titanium content the smaller were the pores. However, the smaller pores were lost as a result of sintering processes at higher temperatures, so that by 1000 °C only macroporosity remained. This resulted in the oxides with greater titanium content (and smaller pores) losing a large proportion of their surface area by 1000 °C.

XPS showed that the titanium ion was in a modified state in the mixed oxides; the titanium cations were in an electron-deficient environment producing enhanced surface acidity. These conclusions were supported by the ammonia TPD experiments which showed that the incorporation of titanium into an alumina matrix produced sites with stronger acidity than the pure oxides. The mixed oxides were found to have greater density of acid sites than alumina and both density and strength of the acid sites were found to increase with titanium content. The Lewis sites density was found to increase with titanium content and the density of Brønsted sites was found to reach a maximum by 10% titanium content. This work has shown that single-phase alumina–titania solid acids have both stronger acid sites and greater acid-site density. This, coupled with the their high surface area, has produced materials with an even greater number of acid sites per gram, making them useful solid acids materials.

Acknowledgements

The authors thank Dr David R. Pyke for the helpful discussions and advice given. We also acknowledge the assistance given by other members of the group, C.R. Werrett and R.C. Reynolds for running the XPS analysis, D. Croci for carrying out the surface area and porosity measurements and K.K. Mallick for DTA–TG and XRD experiments.

References

1. K. TANABE, M. MISOSN, Y. ONO and H. HATTORI, "New Solid Acids and Bases, Their Catalytic Properties" (Elsevier, Oxford, 1989).
2. M. R. MOSTAFA, A. M. YOUSSEF and S.M. HASSAN, *Mater. Lett.* **12** (1991) 207.
3. J. A. MONTOYA, J. M. DOMINGUEZ, J. NAVARRETTE I. SHIFTER, T. VIVEROS, D. CHADWICK and K. ZHENG, *J. Sol-Gel Sci. Technol.* **2** (1994) 431.

4. WEI ZHAOBIN, XIN QIN, GUO XIEXIAN, E.L. SHAM, P. GRANGE and B. DELMON, *Appl. Catal.* **63** (1990) 305.
5. P. R. SILVY, F. LOPEZ, Y. ROMERO, E. REYES, V. LEÓN and R. GALIASSO, *Stud. Surf. Sci. Catal.* **91** (1995) 281.
6. J. RAMIREZ, L. RUIZ-RAMIREZ, L. CEDENO, V. HARLE, M. VRINAT and M. BREYSSE, *Appl. Catal. A* **93** (1993) 163.
7. J. RAMIREZ, T. KLIMOVA, Y. HUERTA and J. ARACIL, *ibid.* **118** (1994) 73.
8. J. C. YORI, J. C. LUY and J. M. PARERA, *Appl. Catal.* **41** (1988) 1.
9. K. JIRÁTOVÁ and J. ROCEK, *Coll. Czech. Chem. Commun.* **52** (1987) 48.
10. E. RODENAS, T. YAMAGUCHI, H. HATTORI and K. TANABE, *J. Catal.* **69** (1981) 434.
11. C. LAHOUSSE, F. MAUGÉ, J. BACHELIER and J-C. LAVALLEY, *J. Chem. Soc. Farad. Trans.* **91** (1995) 2907.
12. B. M. REDDY, M. V. KUMAR, E. P. REDDY and S. MEHDI, *Catal. Lett.* **36** (1996) 187.
13. K-N. P. KUMAR, *Appl. Catal. A* **119** (1994) 163.
14. DONG JIN SUH and TAE-JIN PARK, *Chem. Mater.* **8** (1996) 509.
15. J. B. MILLER, S. E. RANKIN and E. I. KO, *J. Catal.* **148** (1994) 673.
16. L. L. MURRELL, N. C. DISPENZIERE Jr. and K. S. KIM, in R.T.K. Baker and L. L. Murrell (eds), "Novel Materials in Heterogeneous Catalysis" (American Chemical Society, Washington, 1990) p. 97.
17. A. K. BHATTACHARYA, D. R. PYKE, R. REYNOLDS, G. S. WALKER and C. R. WERRET, *J. Mater. Sci. Lett.* **16** (1997) 1–3.
18. C. R. WERRETT, A. K. BHATTACHARYA and D. R. PYKE, *Surf. Interface Anal.*, to be published.
19. B. C. LIPPENS and J. J. STEGGERDA, in "Physical and Chemical Aspects of Adsorbents and Catalysts", edited by B.G. Linsen (Academic Press, London, 1970) Ch. 4.
20. K. WEFERS and G. M. BELL, ALCOA Research Laboratories Tech. Paper No. 19 (1972).
21. C. J. BRINKER and G. W. SCHERER, "Sol-Gel Science, The Physics and Chemistry of Sol-Gel Processing", (Academic Press, London, 1990).
22. M. E. STRAUMANIS, T. EJIMA and W.J. JAMES, *Acta Crystallogr.* **14** (1961) 493.
23. R. J. H. CLARK, in "Comprehensive Inorganic Chemistry", Vol. 3, edited by J. C. Bailar, H. J. Emeléus, R. Nyholm and A.F. Trotman-Dickenson (Pergamon Press, Oxford, 1973) p. 377.
24. J. A. ANDERSON and C. H. ROCHESTER, *J. Chem. Soc., Farad. Trans.* 1, **82** (1986) 1911.
25. B. E. YOLDAS, *J. Non-Cryst. Solids* **63** (1984) 145.
26. I. A. MONTOYA, T. VIVEROS, J. M. DOMÍNGUEZ, L. A. CANALES and I. SCHIFTER, *Catal. Lett.* **15** (1992) 207.
27. O. RODRIGUEZ, F. GONZÁLEZ, P. BOSCH, M. PORTILLA and T. VIVEROS, *Catal. Today* **14** (1992) 243.
28. Y. POLEVYA, J. SAMUEL, M. OTTOLENGHI and D. AVNIR, *J. Sol–Gel Sci. Technol.* **5** (1995) 65.
29. J. C. LAVALLEY, *Catal. Today* **27** (1996) 377.
30. T. IIZUKA and K. TANABE, *Bull. Chem. Soc. Jpn* **48** (1975), 2527.
31. T. A. GORDYMOVA and A. A. DAVYDOV, *Zh. Prikl. Spektrosk.* **39** (1983) 621.
32. F. KAPTEIJN, L. SINGOREDJO, M. VAN DRIEL, A. ANDREÏNI, J. A. MOULIJN, G. RAMIS and G. BUSCA, *J. Catal.* **150** (1994) 105.
33. G. RAMIS, LI YI and G. BUSCA, *Catal. Today* **28** (1996) 373.
34. A. A. DAVYDOV, "Infrared Spectroscopy of Adsorbed Species on the Surface of Transition Metal Oxides" (Wiley, Chichester, 1990).
35. Z. LIU, J. TABORA and R. J. DAVIS, *J. Catal.* **149** (1994) 117.
36. I. OLEFJORD, H. J. MATHIEU and P. MARCUS, *Surf. Interface Anal.* **15** (1990) 681.
37. M. C. BALL and A. H. NORBURY, "Physical Data for Inorganic Chemists" (Longman, London, 1974) p. 175.

Received 10 March
and accepted 1 May 1997